Available online at www.sciencedirect.com
ScienceDirect
Applied Catalysis B: Environmental 81 (2008) 97–104
APPLIED CATALYSIS B: ENVIRONMENTAL
www.elsevier.com/locate/apcatb

Effect of pretreatment on the activity of Ni catalyst for CO removal reaction by water–gas shift and methanation

Sung Ho Kim [a], Suk-Woo Nam [b], Tae-Hoon Lim [b], Ho-In Lee [a,*]

[a] School of Chemical and Biological Engineering & Research Center for Energy Conversion and Storage, Seoul National University, Seoul 151-744, Republic of Korea
[b] Center for Fuel Cell Research, Korea Institute of Science and Technology, Seoul 136-791, Republic of Korea

Received 11 December 2006; received in revised form 17 November 2007; accepted 12 December 2007
Available online 23 December 2007

Abstract

An Ni metal catalyst manufactured by the tapecasting method for use as a structural catalyst did not exhibit catalytic activity for the carbon monoxide (CO) removal reaction. However, the catalyst pretreated by an oxidation and reduction process showed superior activity for CO removal via water–gas shift and methanation, resulting in a decrease of the CO concentration to below 1% in reformate gas. The catalytic activity was generated by the reorganization of the surface structure of Ni metal, and enhanced by surface oxygen intermediates such as $Ni(OH)_2$ and NiOOH promoted by NiO oxidized incompletely after the pretreatment. After the reorganization process induced by the pretreatment, the Ni metal on the surface was converted to active Ni and NiO which played the role of a promoter.

Keywords: Fuel processor; Disk type; Carbon monoxide; Water–gas shift; Methanation

1. Introduction

Due to the increasing interest in hydrogen energy, especially fuel cell technology, the generation and storage of hydrogen is expected to become an important avenue of research. For this purpose, the conventional reforming reaction needs to be adapted to the fuel cell in order for it to function as a fuel processor. The reforming of hydrocarbons (methane, LPG, LNG, and so on) has traditionally been used as a sub-step for ammonia synthesis, methanol synthesis, and Fisher–Tropsch synthesis [1,2], but in recent years, this process has also been developed as a fuel source to supply hydrogen to fuel cells. In the conventional reforming reaction, the concentrations of carbon monoxide and carbon dioxide, as well as that of hydrogen, were important variables in the Fisher–Tropsch process. However, it is now important for the reforming process to apply the fuel source, H_2, to the fuel cell system under specific reaction conditions. Water–gas shift (WGS) has been studied to generate syngas from the reaction between carbon/CO and steam. In a fuel cell system, WGS is conducted to reduce the high concentration of CO naturally contained in reformate gas. In a polymer electrolyte membrane fuel cell (PEMFC), Pt is used as an active catalyst, but it can easily be poisoned by CO species adsorbed on the Pt active sites. Therefore, preferential oxidation process (PROX) [3,4] has been introduced to purify the CO-containing reformate gas by adding air, as well as WGS. The methanation reaction has also been used as an alternative to PROX to remove the carbon monoxide contained in reformate gas after WGS step, in which it is not necessary to introduce air, as in the PROX process. A fuel processor is composed of the above reaction process steps (reforming, water–gas shift, and PROX or methanation reaction) and supplies CO-free hydrogen gas to a PEMFC.

The first report on WGS was published in 1888 [5] and explained how the reaction of carbon monoxide and steam produced H_2 and CO_2 over red-hot refractory material. Since then, researchers at BASF [6,7], as part of the development of an ammonia synthesis process, tested the suitability of several kinds of metallic oxides for WGS. Fe_2O_3-Cr_2O_3 type catalysts were found by these researchers and have since been used in commercial high temperature water–gas shift (HTS). In the early 1960s, the WGS process in commercial plants was divided into two separate steps, which were composed of HTS using an Fe_2O_3-Cr_2O_3 catalyst [8,9] and low temperature WGS (LTS) using a $Cu/ZnO/Al_2O_3$ catalyst [10,11]. In this way, the

* Corresponding author. Tel.: +82 2 880 7072; fax: +82 2 888 7295.
E-mail address: hilee@snu.ac.kr (H.-I. Lee).

0926-3373/$ – see front matter © 2007 Elsevier B.V. All rights reserved.
doi:10.1016/j.apcatb.2007.12.009

10–20% of CO contained in the gas was reduced after the reforming process to 3–5% operating at temperatures ranged from 300 to 500 °C by HTS and then to below 1% carrying out at lower temperatures (180–300 °C) by LTS [12]. The conventional catalyst and process have been applied into a recent fuel processing system [13–15].

Ni metal, which has been applied widely in methanation reaction [16] and recently in WGS [17], was sintered to manufacture a structural catalyst and was pretreated to activate for removing high concentration of carbon monoxide. We tried to reduce 15% CO used in this study to below 1% with a one-step reaction instead of the two-step water–gas shift (HTS and LTS) process. A lot of hydrogen may be converted to CH_4 by methanation over Ni bulk catalyst, resulting in consumption of the hydrogen supplied to the fuel cell. The activity of bulk Ni catalyst will be presented, and the properties of the catalyst will be discussed by various characterization methods.

In a fuel processor, the WGS process requires a large volume, ca. 70 vol% of the whole processor system [18], which is one of the barriers to develop an on-board fuel processor. In order to overcome this problem, we have developed a new WGS catalyst for a miniaturized on-board fuel processor system.

2. Experimental

2.1. Preparation of structural catalyst using Ni metal

A slurry containing a mixture of solvent (water), binder (Methyl Cellulose #1,500, Junsei Chemical Co., Japan), plasticizer (Glycerol, Junsei Chemical Co., Japan), defoamer (SN-154, San Nopco Korea), deflocculant (Cerasperse-5468, San Nopco Korea), dispersant (polyacrylic acid) and Ni metal powder (INCO. #255, INCO) was ball milled for 15 h [19]. Then, polyethylene oxide was added to the slurry and the ball milling continued for 6 h. Then, very small amounts of methyl cellulose, sodium carboxyl methyl cellulose as a binder, and isopropyl alcohol as a de-airing agent were added to the slurry and ball milling was conducted for a further 1 h. In order to eliminate the air from the slurry after the third ball milling process, a vacuum pump and stirring equipment were used. A green sheet was made by means of a doctor blade with the slurry, and then it was dried sufficiently at ambient temperature. The Ni green sheet was sintered at 1050 °C in an H_2/Ar atmosphere. Then, the sintered Ni metal was cut into disk-type catalyst with an inner diameter of 16 mm and an outer diameter of 48 mm by means of a laser. The thickness of the Ni disk was ca. 0.75 mm, and their porosity measured by a mercury porosimeter was ca. 50%. Fig. 1 shows the entire procedure of the tapecasting method (Fig. 1 (1)) and the shape of the disk-type Ni catalyst (Fig. 1 (2)). Fig. 2 (1) and (2) shows the surface morphology of the pure Ni metal and the morphology of the pure Ni sintered at high temperature, respectively.

2.2. Reaction system and activity test

The reactor for the structural catalyst was made of stainless steel in order to withstand high temperature. The composition

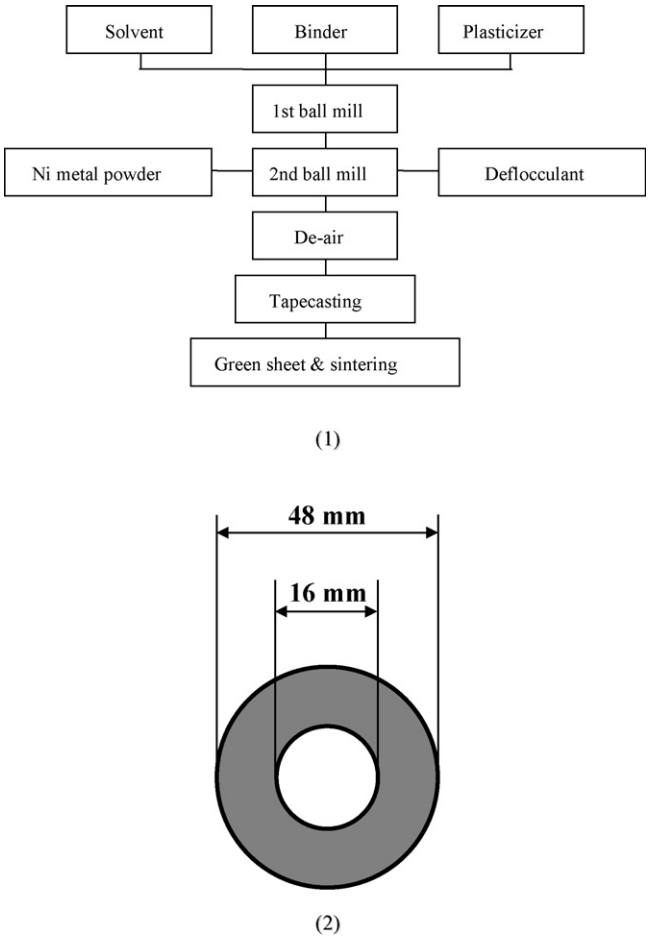

Fig. 1. (1) An entire procedure of tapecasting method to manufacture a structural catalyst using Ni metal. (2) A shape of disk-type porous Ni metal catalyst.

of the standard reactant that was used to simulate the gas reformed from an autothermal methane reforming process was 15% CO, 40% H_2, and 10% CO_2 in N_2 balance of dry base. The reactant gas (400 ccm) was passed through an evaporator for steam supply and introduced vertically into the reactor with a steam/CO ratio of 5 for CO removal with one step, and flowed in parallel over the catalyst layer as shown in Fig. 3. An Inconel sheet layer was used to define the flow path.

The flow rate of the reformate gas used as the reactant was controlled by a mass flow controller, and the amount of steam was controlled by adjusting the evaporator temperature. A line heater was employed at 250 °C to maintain the steam flowing without condensation from the evaporator to the reactor inlet.

Analyses of the product mixture of CO, CH_4, CO_2 and O_2 gases were conducted by a CO analyzer (SIEMENS, ULTRAMAT 23).

2.3. Characterization of the catalyst

The surface morphology of the catalyst was observed using scanning electron microscopy (SEM, FEI XL-30 FEG) and its crystal structure was measured by X-ray diffraction (D/MAX-IIIA X-ray diffractometer, Rigaku) with CuKα radiation. The BET surface area was measured by nitrogen adsorption–

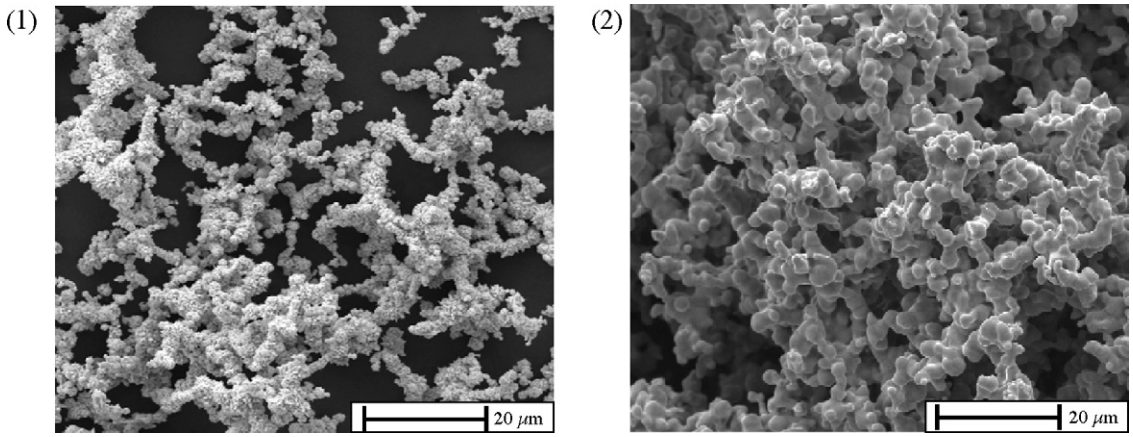

Fig. 2. SEM images: (1) morphology of Ni metal powder. (2) Morphology of Ni metal sintered at 1050 °C with H_2/Ar.

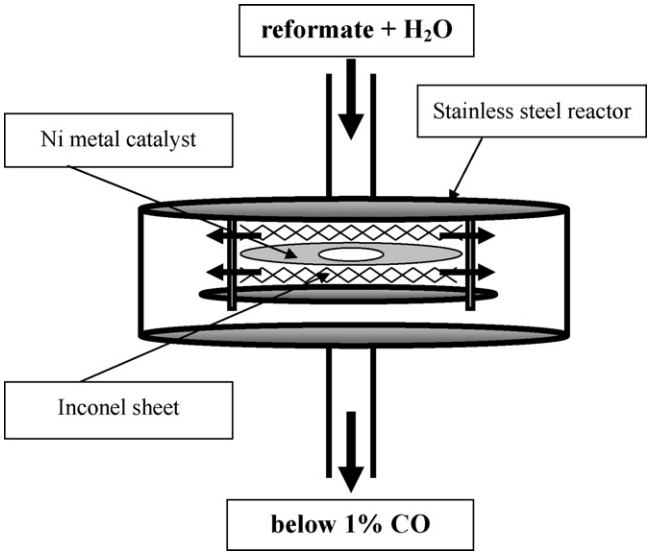

Fig. 3. A schematic diagram of reactor and reaction system.

desorption using a Micromeritics ASAP 2010 instrument and the porosity of the Ni metal catalyst was measured by means of a mercury porosimeter using Archimedes' principle (ASTM, C373-88). The chemisorption area was determined by hydrogen adsorption–desorption experiment using a Micromeritics ASAP 2020 apparatus. The XPS analysis of the catalyst was carried out at room temperature with a VGESCALAB 220i-XL spectrometer (Fisons). The residual pressure in the spectrometer was in the range of 1.3–6.5 $\times$ 10^{-7} Pa. A monochromated Al anode (energy of the AlKα line, 1486.6 eV), powered at 10 keV and 20 mA, was used as the X-ray source. The XPS spectrum of all of the samples was calculated with respect to the Au $4f_{7/2}$ core level, 84.0 eV.

3. Results and discussion

3.1. Effect of oxidation process in pretreatment of Ni metal catalyst

The pretreatment of the Ni metal catalyst before the activity test was proceeded by oxidation process with 400 ccm air at 600 °C and subsequent reduction process with steam (at 77.5 °C) and 400 ccm reformate gas for 0.5 h at 500 °C.

An XRD analysis was conducted to analyze the state of the catalyst after oxidation at various times and after the CO removal reaction by WGS and methanation. It was considered that the state of the catalyst after the CO removal reaction was representative of that of a practical catalyst condition under the real reaction conditions. N_2 was constantly purged to sustain the state of the catalyst after the reaction during the decrease in the reactor temperature. In Fig. 4, the XRD peak positions (by 2θ in degree) of Ni were 44.50, 51.84 and 76.36, and those of NiO were 37.28, 43.32, 62.9, 75.47 and 79.5. From the results of Fig. 4, the NiO peaks were detected in all of the samples after the oxidation process, but Ni was observed in addition to NiO because of the incomplete oxidation of the catalyst. As the oxidation time of the Ni metal increased, the peak intensity of NiO increased, while that of Ni decreased. The NiO shown in Fig. 4 (a′–e′) was not reduced completely and a small amount of NiO remained with Ni in the catalyst even after the CO removal

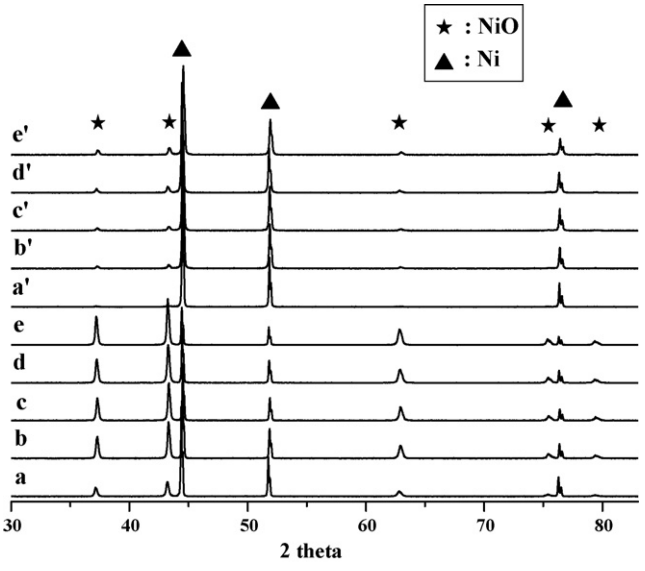

Fig. 4. The results of XRD; after oxidation for (a) 0.5 h, (b) 1 h, (c) 2 h, (d) 4 h, and (e) 8 h at 600 °C with air; after reaction over the reduced Ni metal of (a′) a, (b′) b, (c′) c, (d′) d, and (e′) e at 500 °C with reformate gas and steam.

reaction. The peak intensity of NiO after the reaction was also increased in proportion to the oxidation time, which means that the concentration of NiO was increased in the pretreated catalyst.

The Ni metal catalyst has a filamentary structure and irregular surface (see Fig. 2 (1)). The particles of the sintered Ni metal powder were networked with each other and had an average pore size distribution of 3–5 μm (see Fig. 2 (2)). As well as the Ni metal particles being mutually interconnected, the structural catalyst was porous as shown in SEM image of Fig. 5 (1). Also the surface of the Ni metal became smooth and stabilized due to the high sintering temperature, i.e. 1050 °C. The SEM images of Fig. 5 (2) and (2′) show the surface of the Ni metal catalyst oxidized at 600 °C for 2 h with air. Even though the Ni metal catalyst was oxidized for 2 h, the XRD patterns in Fig. 4 show that Ni and NiO homogenously co-existed and the SEM images in Fig. 5 (2) and (2′) show that surface expansion occurred due to the difference between the lattice constants of Ni and NiO in the oxidized catalyst. It was observed in Fig. 5 (3) and (3′) that the pores on the catalyst surface of the oxidized Ni reduced by reformate gas and steam were well developed. While the expanded surface of the oxidized Ni metal catalyst was reduced to Ni, only oxygen was extracted from the NiO and the structure of the expanded Ni remained porous, as shown in Fig. 5 (3) and (3′). The pores were generated by the restructuring of the smooth surface of the Ni metal catalyst during the pretreatment, oxidation and reduction processes. It can be assumed within a category of catalysis that the non-catalytic surface of Ni metal of Fig. 5 (1) and (1′) became unstable and that this led to the formation of the active structures of Fig. 5 (3) and (3′), such as the kinks, steps and terraces through the pretreatment of the Ni surface, which are the role of the catalytic active sites.

The results of the N_2 adsorption analysis demonstrate that the specific surface area (2.1 m^2/g) of the pretreated Ni metal catalyst was larger than that of the pure Ni metal (0.4 m^2/g), and it was supposed that the pretreatment of the catalyst might have an effect on the catalytic activity by reorganizing the smooth surface of Ni metal such that it became porous. H_2-chemisorption analysis was conducted as evidence on the formation of new active sites. The metallic surface areas of the pretreated Ni and pure Ni were 0.0421 m^2/g and 0.0016 m^2/g, respectively. In comparison with BET surface area, the chemisorption result of the pretreated catalyst showed much larger value than that of pure Ni suggesting surface reorganization.

The activity test of the pretreated catalyst was performed by cooling it down from 500 °C to 350 °C to remove CO by WGS and methanation reactions, in which the flow rate of reformate gas was 400 ccm and the ratio of steam to carbon monoxide was 5. The catalytic activity of the pretreated Ni metal was measured to investigate the effect of NiO and Ni on the removal of CO. Fig. 6 (1) shows that the reaction window to remove CO widens with increasing oxidation time of the Ni metal catalyst. While the pure Ni metal catalyst had no effect on the reaction, the pretreated Ni metal catalyst containing NiO showed strong activity. The hidden catalytic active sites of the pure Ni metal can be emerged by the pretreatment process, followed by oxidation and reduction, and NiO plays a role in the removal of CO by acting as a promoter. Thermodynamically [20], 15% of CO cannot be reduced to less than 1% CO solely by WGS. However, the thermodynamic restriction was overcome by applying the concept of methanation to WGS under our condition. In WGS reaction, the temperature dependence should be considered. However, the temperature dependence was not mentioned specifically in the text because methanation occurred simultaneously with WGS giving their own respective

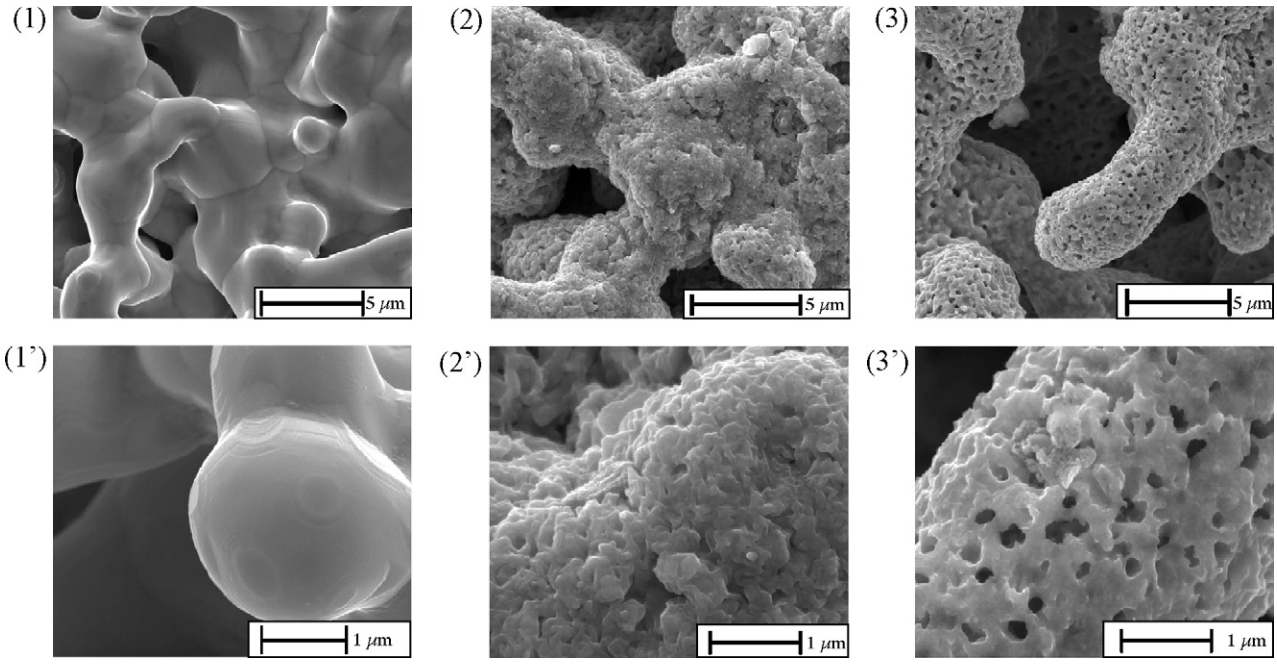

Fig. 5. SEM images of Ni metal catalyst; (1) and (1′), pure Ni metal; (2) and (2′), an oxidized surface of (1) and (1′); (3) and (3′), a reduced surface of (2) and (2′).

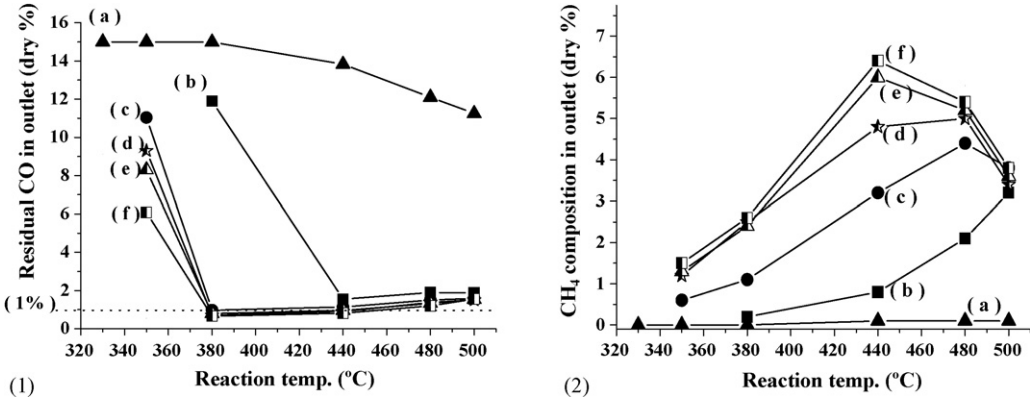

Fig. 6. The results of activity test; (1) residual CO (dry%) and (2) methane composition in outlet over the Ni metal catalyst oxidized at 600 °C for (a) 0.5 h, (b) 1 h, (c) 2 h, (d) 4 h, and (e) 8 h with air.

effects on the CO removal reaction. The results, therefore, could not be interpreted by only WGS.

When Ni catalyst was oxidized for 0.5 h and 2–8 h, 15% of carbon monoxide was decreased and reached to 1–2% at 440–500 °C and to below 1% at 380–440 °C, respectively. The amount of residual carbon monoxide decreased with increasing oxidation time. The catalytic activity of pretreated Ni was dependent on oxidation time, but the pretreated catalysts showed similar activity at 440–500 °C. From the result of methane composition shown in Fig. 6 (2), the methane composition was increased by increasing oxidation time at 440 °C showing similar residual CO concentration in all the pretreated samples. It was observed that the methanation reaction at higher than 440 °C was enhanced by the oxidation of Ni metal catalyst even though the catalytic activity for removing carbon monoxide gradually increased with increasing oxidation time.

The high concentration of carbon monoxide could be reduced to below 1% by the pretreatment of the Ni metal catalyst in order to overcome the thermodynamic restriction of WGS by positively employing the methanation reaction. The one step process for carbon monoxide removal using the pretreated Ni metal catalyst will enable the minimization of on-board fuel processing system by eliminating the need for the two step WGS process which makes up 70 vol% of the total fuel process.

3.2. Effect of reduction process in pretreatment of Ni metal catalyst

In this section, various reduction conditions were used to investigate the effect of NiO on the surface of the pretreated Ni metal catalyst for WGS and methanation in the CO removal reaction. The oxidation process was carried out at 600 °C for 2 h under an air atmosphere of 400 ccm for all of the samples. For the reduction process, the flow rate of reformate gas used as a reducing agent was fixed at 400 ccm (CO 15%, H_2 40%, CO_2 10% and N_2 balance) and passed though an evaporator to introduce steam (at 77.5 °C).

Fig. 7 shows the state of the pretreated catalyst after the CO removal reaction by WGS and methanation under various reduction conditions. In the XRD results of Fig. 7, when the reduction time was lengthened from 0.5 h (a) to 1 h (b) at 500 °C, the peak intensity of NiO decreased slightly. When the reduction temperature was increased to 550 °C (c) and 600 °C (d), the peak of NiO almost disappeared, indicating that there was a decrease of the NiO concentration.

The Ni $2P_{3/2}$ XPS spectra for all of the samples after the carbon monoxide removal reaction are shown in Fig. 8. These peaks are in good agreement with the general NiO peak

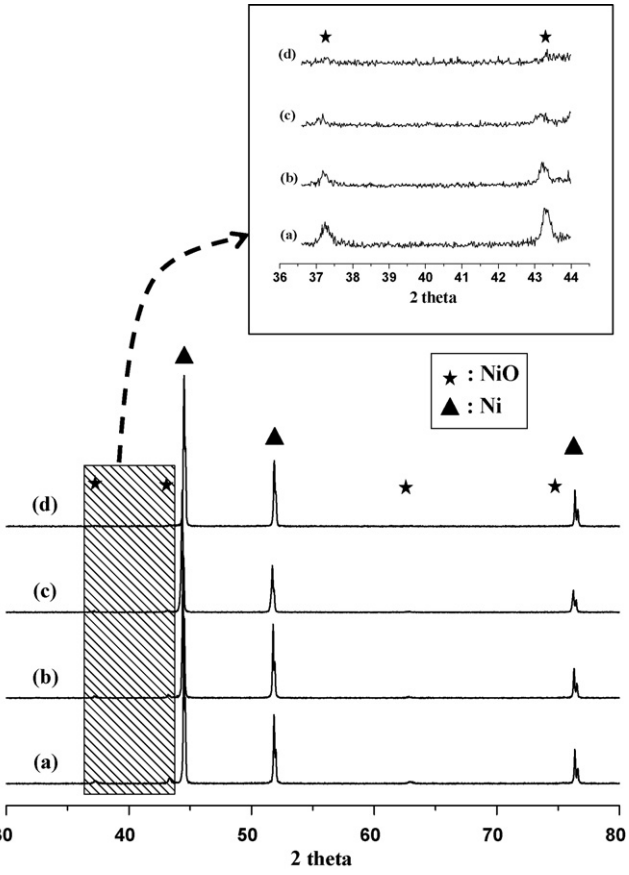

Fig. 7. The results of XRD after CO removal reaction by WGS and methanation over the reduced Ni metal catalyst (a) at 500 °C for 0.5 h, (b) at 500 °C for 1 h, (c) at 550 °C for 1 h, and (d) at 600 °C for 1 h.

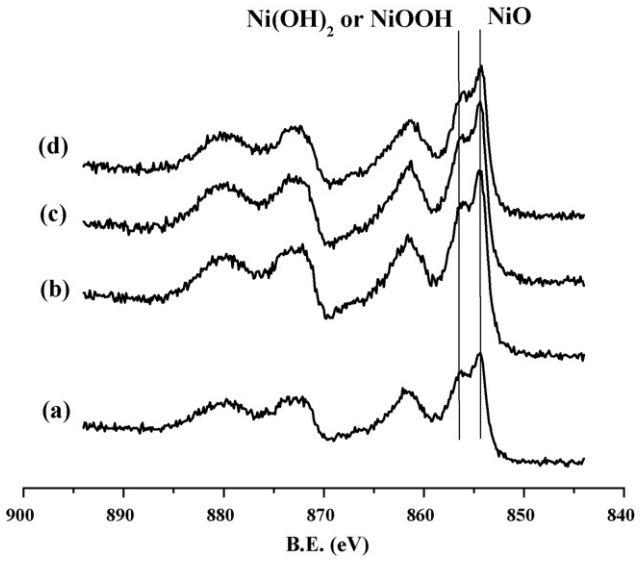

Fig. 8. The results of XPS of Ni2p core level after CO removal reaction by WGS and methanation over the reduced Ni metal catalyst (a) at 500 °C for 0.5 h, (b) at 500 °C for 1 h, (c) at 550 °C for 1 h, and (d) at 600 °C for 1 h.

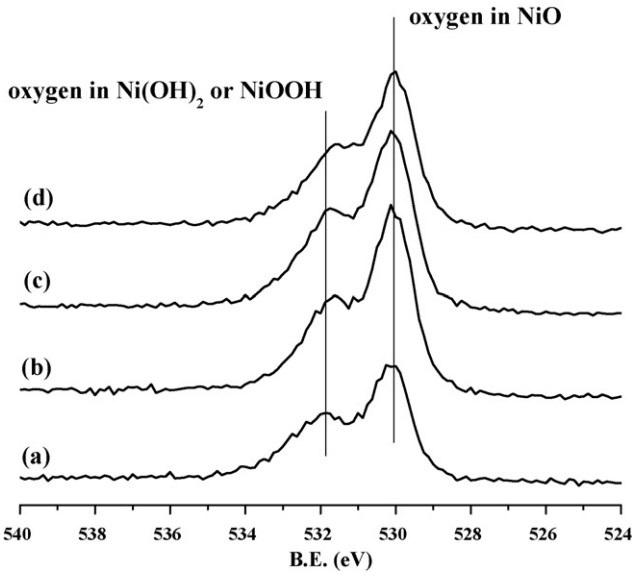

Fig. 9. The results of XPS of O1s core level after CO removal reaction by WGS and methanation over the reduced Ni metal catalyst (a) at 500 °C for 0.5 h, (b) at 500 °C for 1 h, (c) at 550 °C for 1 h, and (d) at 600 °C for 1 h.

spectrum [21,22] and they are expected to have an effect on WGS by Ni–$(OH)_2$ and on the methanation by NiO. Fig. 9 shows the XPS spectra of O_{1s} core level of Ni metal after the reaction and all of the samples present two different peaks. The main peak of O_{1s} is observed at ca. 530 eV and an additional shoulder appears at ca. 532 eV. The higher binding energy shoulder is attributed to the oxygen vacancies or O^- species (hydroxyl group, –OH) and the lower peak (at 530 eV) corresponds to the oxygen in NiO [23,24]. Surface oxygen intermediates such as Ni–$(OH)_2$ or Ni–OOH [22,24] which is shown at 532 eV are formed on the surface of the pretreated Ni metal, and are expected to have some catalytic effect on the carbon monoxide removal reaction [25].

Fig. 10 (1) shows that, when the oxidized catalyst was reduced at 500 °C for 1 h, its catalytic activity on the carbon monoxide removal showed a similar performance at over 440 °C, but was different at below 440 °C as compared with the catalyst reduced at 500 °C for 0.5 h. The residual carbon monoxide in the outlet at 380 °C, in the case of the catalyst reduced at 550 °C and 600 °C for 1 h, was more abundant than that in the case of the catalyst reduced at 500 °C for 0.5 h. However, at temperatures over 440 °C, the amount of residual carbon monoxide remained almost constant for all the samples. Fig. 10 (2) shows that NiO does not affect the WGS, but has some effect on the methanation reaction. The more NiO the pretreated catalyst contained, the more methane there is produced.

Nickel has been investigated as an effective catalyst for the methanation reaction [16], which is carried out using a CO/H_2 gas mixture in the temperature range of 500–700 K. It has been widely accepted that the reaction is promoted by the active carbonaceous carbon produced from the dissociation of the C–O bond [26–28]. The Ni catalysts are also active but not selective for WGS [29,17]. Several mechanisms have been proposed for WGS, even though no direct evidence has yet been established for any of them. Among these mechanisms, the

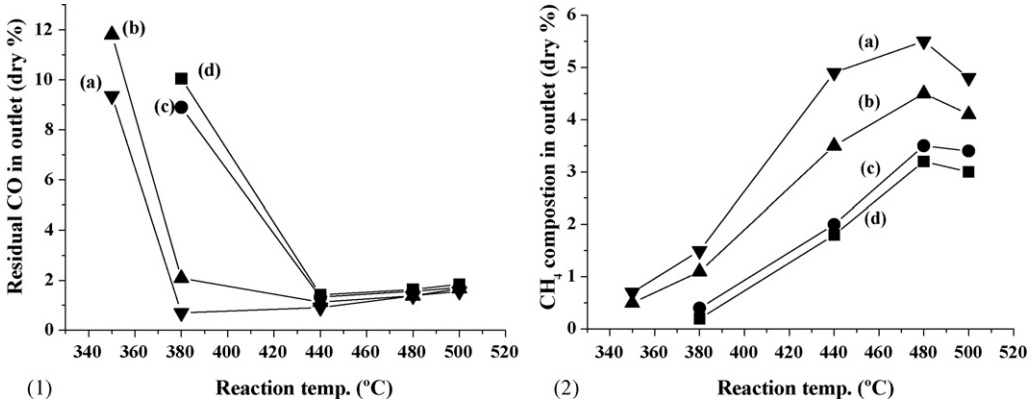

Fig. 10. The results of activity test: (1) residual CO (dry%) and (2) methane composition in outlet over the reduced Ni metal catalyst (a) at 500 °C for 0.5 h, (b) at 500 °C for 1 h, (c) at 550 °C for 1 h, and (d) at 600 °C for 1 h.

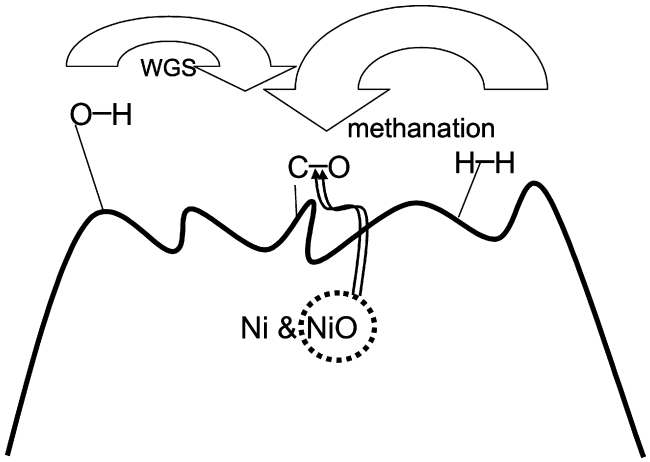

Scheme 1. The schematic diagram of carbon monoxide removal reaction by water–gas shift and methanation over the pretreated Ni metal catalyst.

associative mechanism, which is similar to the mechanism for copper catalysts [30] seems to be applicable to the Ni catalyst [29]. Water dissociation on the partially oxidized Ni surface provides the initial step for WGS and produces adsorbed hydroxyl group and atomic hydrogen. The hydroxyl group then reacts with adsorbed carbon monoxide to form an intermediate and eventually decomposes into carbon dioxide and hydrogen.

Also, according to Wheeler et al. [31], Ni gave the highest carbon monoxide conversion and resulted in the undesired formation of carbon intermediate which facilitated the methanation reaction of carbon monoxide. In addition, Dongare et al. [23] reports that surface O^- species (presented in high B.E. in XPS results of Fig. 9) hints that the high oxygen mobility might be expected to influence the catalytic properties and these surface oxygen species also increased with the amount of NiO. Even though oxygen on the Ni surface is likely to lead to the formation of –OH intermediate [32,33] which constitutes the catalytically active site of the proposed regenerative mechanism of WGS [29,34–36], the methanation reaction on the pretreated Ni catalyst might be promoted by the presence of O_{ads} species which are more reactive than the –OH surface groups [32,33]. Scheme 1 shows a schematic diagram of the CO removal reaction by WGS and methanation over the pretreated Ni metal catalyst.

That is, the NiO in the pretreated catalyst weakens the C–O bond. This is the reason that a high NiO concentration in the pretreated catalyst increases the methane composition in the outlet. Before the C–O adsorbed on the catalyst surface reacts with the –OH group, the C–O bond, which is weakened by the active oxygen on Ni, preferentially reacts with H_2. Due to these interactions, the NiO produced by the pretreatment facilitates the formation of the surface carbon intermediates which are easily hydrogenated to produce methane.

4. Conclusions

High CO concentration (15% in dry condition) in reformate gas could be reduced to below 1% CO concentration by only one-step process. The catalytic activity in the pretreated Ni metal catalyst was attributed to the reorganization of the surface structure of Ni. NiO in the pretreated catalyst weakened the C–O bond, and surface carbon intermediate facilitated by NiO was easily hydrogenated to produce methane.

Considering that the pretreated Ni metal catalyst is substituted for the WGS catalyst of a fuel processor, it is possible to reduce the scale of the system in order to make a portable power system. The methanation reaction, which consumes the hydrogen used as the fuel source of the fuel cell, must be suppressed to enhance the hydrogen energy yield.

Acknowledgements

This work was financially supported by the Center for Fuel Cell Research of Korea Institute of Science and Technology, and by the ERC program of MOST/KOSEF (Grant No. R11-2002-102-00000-0).

References

[1] J.R. Rostrup-Nielsen, I. Dybkjaer, K. Aasberg-Petersen, Prepr. ACS Petr. Chem. Div. 45 (2) (2000) 186.
[2] J.R. Rostrup-Nielsen, Catal. Today 71 (2002) 243.
[3] C.R. Jung, J. Han, S.W. Nam, T.-H. Lim, S.-A. Hong, H.-I. Lee, Catal. Today 93-95 (2004) 183.
[4] W.-S. Shin, C.R. Jung, J. Han, S.W. Nam, T.-H. Lim, S.-A. Hong, H.-I. Lee, J. Ind. Eng. Chem. 10 (2004) 302.
[5] C. Rhodes, G.J. Hutchings, A.M. Ward, Catal. Today 23 (1995) 43.
[6] BASF, B. Anilin and S. Fabrik. Patents: EP 21151/1911; GP 254571/1911; 256296/1911; 259870/1911; 265295/1912.
[7] C. Bosch, W. Wild, Canadian Patent 153 (1914) p. 379.
[8] Y. Lei, N.W. Cant, D.L. Trimm, J. Catal. 239 (2006) 227.
[9] S. Natesakhawat, X. Wang, L. Zhang, U.S. Ozkan, J. Mol. Catal. A: Chem. 260 (2006) 82.
[10] G. Jacobs, S. Ricote, B.H. Davis, Appl. Catal. A 302 (2006) 14.
[11] H. Yahiro, K. Murawaki, K. Saiki, T. Yamamoto, H. Yamaura, Catal. Today 126 (2007) 436.
[12] V. Galvita, K. Sundmacher, Chem. Eng. J. 134 (2007) 168.
[13] G. Kolb, J. Schurer, D. Tiemann, M. Wichert, R. Zapf, V. Hessel, H. Lowe, J. Power Sources 171 (2007) 198.
[14] Y.T. Seo, D.J. Seo, J.H. Jeong, W.L. Yoon, J. Power Sources 163 (2006) 119.
[15] Y.T. Seo, D.J. Seo, J.H. Jeong, W.L. Yoon, J. Power Sources 160 (2006) 505.
[16] S. Takenak, T. Shimizu, K. Otsuka, Int. J. Hydrogen Energy 29 (2004) 1065.
[17] Y. Li, Q. Fu, M.F. Stephanopoulos, Appl. Catal. B 27 (2000) 179.
[18] T.A. Semelsberger, R.L. Borup, Int. J. Hydrogen Energy 30 (2005) 425.
[19] S.-A. Hong, I.-H Oh, T.-H. Lim, S.W. Nam, H.Y. Ha, S.-P. Yoon, J. Han, K.-S. Lee, KR patent, 2003-0070725.
[20] T. Utaka, T. Takeguchi, R. Kikuchi, K. Eguchi, Appl. Catal. A 246 (2003) 117.
[21] M.W. Roberts, R.St.C. Smart, J. Chem. Soc. Faraday I 80 (1984) 2957.
[22] A.P. Grosvenor, M.C. Biesinger, R.St.C. Smart, N.S. McIntyre, Surf. Sci. 600 (2006) 1771.
[23] M.K. Dongare, K. Malshe, C.S. Gopinath, I.K. Murwani, E. Kemnitz, J. Catal. 222 (2004) 80.
[24] M. Schulze, R. Reissner, M. Lorenz, U. Radke, W. Schnurnberger, Electrochim. Acta 44 (1999) 3969.
[25] J.-H. Kim, H.-I. Lee, Korean J. Chem. Eng. 21 (1) (2004) 116.
[26] N.W. Gupta, V.S. Kamble, R.M. Iyer, J. Catal. 60 (1979) 57.
[27] K.O. Xavier, R. Sreekala, K.K.A. Rashid, K.K.M. Yusuff, B. Sen, Catal. Today 49 (1999) 17.
[28] I.-G. Bajusz, J.G. Goodwin Jr., J. Catal. 169 (1997) 157.

[29] M.S. Spencer, Catal. Today 12 (1992) 453.
[30] G.C. Chinchen, M.S. Spencer, J. Catal. 112 (1988) 325.
[31] C. Wheeler, A. Jhalani, E.J. Klein, S. Tummala, L.D. Schmidt, J. Catal. 223 (2004) 191.
[32] H. Guo, F. Zaera, Surf. Sci. 524 (2003) 1.
[33] W. Li, G.V. Gibbs, S.T. Oyama, J. Am. Chem. Soc. 120 (1998) 9041.
[34] T. Shido, Y. Iwasawa, J. Catal. 141 (1993) 71.
[35] T. Shido, Y. Iwasawa, J. Catal. 136 (1992) 493.
[36] G. Jacobs, P.M. Patterson, V.M. Graham, D.E. Sparks, B.H. Davis, Appl. Catal. A 269 (2004) 63.